Cu_2O: Electrodeposition and Characterization

P. E. de Jongh,* D. Vanmaekelbergh, and J. J. Kelly

Debye Institute, Utrecht University, P.O. Box 80 000, 3508 TA Utrecht, The Netherlands

Received April 21, 1999. Revised Manuscript Received September 20, 1999

Well-defined polycrystalline Cu_2O was electrodeposited on transparent conducting substrates from alkaline Cu(II) lactate solutions. The morphology of the layers could be controlled by choosing the appropriate experimental conditions; the pH and temperature of the deposition solution were especially important. The growth of the oxide involves a thermally activated process, for which an activation energy of 0.8 eV was found. A mechanism for the deposition is proposed. The optical absorption of the electrodeposited oxide in the visible range was much weaker than expected for a direct semiconductor with a band gap of 2.0 eV. Finally, we show that it is possible to grow Cu_2O inside an n-type TiO_2 nanoporous matrix.

Introduction

Cuprous oxide and related materials are the subject of much current interest. Recently, it was reported that excitons could propagate coherently through single crystalline Cu_2O. It might be possible to convert photons into excitons, which could travel through small apertures or small dimension waveguides with little loss to scattering and diffraction. At the end of the path the excitons could be converted back into photons.[1] Another exciting development is a Cu_2O-related material, $CuAlO_2$, that was reported as the first transparent oxide showing appreciable p-type conductivity (up to 1 S/cm).[2] Recently, Cu/Cu_2O-layered nanostructured materials with interesting optoelectronic properties have been prepared by electrodeposition.[3,4] Cu_2O has a direct band gap of 2 eV, which makes it a promising material for the conversion of solar energy into electrical or chemical energy. A drawback in a photoelectrochemical cell is its limited stability in aqueous solutions. Several papers have considered the application of Cu_2O in solid-state photovoltaic cells.[5−7] Recently, water splitting activity was reported in a vigorously stirred, illuminated suspension of Cu_2O particles, although the exact mechanism and the precise role of the oxide are unclear.[8,9]

Cu_2O is p-type due to the presence of Cu vacancies which form an acceptor level 0.4 eV above the valence band. The electrical properties depend strongly on the preparation conditions.[10,11] The oxide is one of the few p-type semiconductors that can be prepared by electrodeposition, i.e., by reduction of metal ions in a suitable electrolyte solution. Electrodeposition is a cheap and simple method, offering control over the stoichiometry and thickness of the layers. Cu_2O has already been deposited on several substrates including Pt, Au, Cu, ITO, and stainless steel.[12−15]

An interesting possibility would be to electrodeposit materials inside a nanoporous matrix. Martin has shown that it is possible to obtain nanoscale structures by growing semiconductors such as TiO_2 and ZnO in porous Al_2O_3 or polycarbonate membranes.[16] Interpenetrated materials have been prepared with an intimite electrical contact between the two components.[17,18] Composite materials consisting of suitable, interpenetrated n- and p-type semiconductors could present a wide range of interesting applications such as electroluminescent devices and solid-state solar cells. Recently, photonic band gap materials have been reported, showing strong localization of the light in a porous semiconductor structure.[19,20] New porous semiconductor materials could be prepared by deposition inside a matrix, followed by removal of the matrix.

In this paper, the electrodeposition of Cu_2O on transparent conducting substrates is described. The

* To whom correspondence should be addressed. E-mail: pjongh@phys.uu.nl.

(1) Snoke, D. *Science* **1996**, *273*, 1351.
(2) Kawazoe, H.; Yasukawa M.; Hyodo, H.; Kurita, M.; Yanagi, H.; Hosono, H. *Nature* **1997**, *389*, 939.
(3) Switzer, J. A.; Maune, B. M.; Raub, E. R.; Bohannan, E. W. *J. Phys. Chem. B* **1999**, *103*, 395.
(4) Bohannan, E. W.; Huang, L.-Y.; Scott Miller, F.; Shumsky, M. G.; Switzer, J. A. *Langmuir* **1999**, *15*, 813.
(5) Briskman, R. N. *Sol. Energy Mater. Sol. Cells* **1992**, *27*, 361.
(6) Fujinaka, M.; Berezin, A. A. *J. Appl. Phys.* **1983**, *54*, 3582.
(7) Olsen, L. C.; Addis, F. W.; Miller, W. *Sol. Cells* **1982**, *7*, 247.
(8) Hara, M; Kondo, T.; Komoda, M.; Ikeda, S.; Shinohara, K.; Tanaka, A.; Kondo, J.; Domen, K. *Chem. Commun.* **1998**, 357.
(9) Ikeda, S.; Takata, T.; Kondo, T.; Hitoki, G.; Hara, M.; Kondo, J. N.; Domen, K.; Hosono, H.; Kawazoe, H.; Tanaka, A. *Chem. Commun.* **1998**, 2158.
(10) Bloem, J. *Philips Res. Rep.* **1958**, *13*, 167.
(11) Pollack, G. P.; Trivich, D. *J. Appl. Phys.* **1975**, *46*, 163.
(12) Tench, D.; Warren, L. F. *J. Electrochem. Soc.* **1983**, *130*, 869.
(13) Rakhshani, A. E.; Varghese, J. *Solar Energy Mater.* **1987**, *15*, 237.
(14) Mukhopadhyay, A. K.; Chakraborty, A. K.; Chatterjee, A. P.; Lahiri, S. K. *Thin Solid Films* **1992**, *209*, 92.
(15) Golden, T. D.; Shumsky, M. G.; Zhou, Y.; Vanderwerf, R. A.; van Leeuwen, R. A.; Switzer, J. A. *Chem. Mater.* **1996**, *8*, 2499.
(16) Martin, C. R. *Science* **1994**, *260*, 1961.
(17) Vanmaekelbergh, D.; Koster, A.; Iranzo Marín, F. *Adv. Mater.* **1997**, *9*, 575.
(18) Tennakone, K.; Kumara, G. R. R. A.; Kumarasinghe, A. R.; Wijayantha, K. G. U.; Sirimanne, P. M. *Semicond. Sci. Technol.* **1995**, *10*, 1689.
(19) Schuurmans, F. J. P.; Vanmaekelbergh, D.; van de Lagemaat, J.; Lagendijk, A. *Science* **1999**, *284*.
(20) Wiersma, D. S.; van Albada, M. P.; van Tiggelen, B. A.; Lagendijk, A. *Phys. Rev. Lett.* **1995**, *74*, 4193.

10.1021/cm991054e CCC: $18.00
Published on Web 12/20/1999

influence of deposition variables, such as temperature, pH, and current density are related to the morphology of the layers. The material is characterized using SEM, XRD, and optical absorption measurements. The photoelectrochemical properties of the electrodeposited layers are discussed elsewhere.[21] In the last section we show that it is possible to grow the Cu_2O in a TiO_2 nanoporous matrix, and we investigate the electrical contact between the two interpenetrated phases.

Experimental Section

Cu_2O layers were electrodeposited on a transparent conducting substrate, fluorine-doped tin oxide (TFO), by reduction of Cu^{2+} from a Cu(II) lactate basic aqueous solution.[15] A total of 45 g of Cu_2SO_4 was dissolved in 75 mL of 88% lactic acid to form the copper lactate complex. A total of 225 mL of a 5 M NaOH aqueous solution was added in small portions to the copper solution. The dark blue solution was stirred overnight, and the pH was adjusted to the desired value using a 5 M NaOH solution.

The Cu_2O was grown either galvanostatically or potentiostatically in a standard three-electrode electrochemical setup using an EG&G PAR 273A potentiostat, a large area platinum counter electrode, and a saturated calomel reference electrode (SCE). Cu_2O can only be electrodeposited in a limited potential range, at pH 9 between approximately −0.1 and −0.6 V vs SCE. The current densities for galvanostatic deposition ranged from 0.05 to 3.0 mA/cm^2. If the current density was too high, the electrodeposition potential was very negative and started to oscillate. During these oscillations probably not only Cu_2O but also Cu is formed.[22] The current density was therefore chosen low enough to avoid oscillations. Two important experimental variables were the pH (in the range 7−13) and the temperature of the electrodeposition solution (10−65 °C).

The Cu_2O layers were characterized by optical absorption spectroscopy, X-ray diffraction, and scanning electron microscopy using a Philips XL30 FEG electron microscope. The thickness of the layers was determined using a Tencor AS500 surface profiler and by analyzing the interference pattern in the absorption spectrum.

Cu_2O was also deposited in 1−2 μm thick nanoporous TiO_2 electrodes, consisting of TiO_2 particles (Degussa P25) with a diameter of 20−30 nm. These nanoporous electrodes were prepared by dip-coating TFO conducting substrates from a 160 g/L TiO_2 suspension and annealing for 2 h at 450 °C under air. The deposition conditions were similar to those for the Cu_2O deposition on bare TFO. In addition to the other techniques, Rutherford Backscattering Spectrometry (RBS) was performed to obtain information about the distribution of the Cu_2O in the TiO_2 electrode. A 2 MeV He^+ beam was used, and the sample surface was tilted at 25° to the incident beam in order to obtain a higher depth resolution.

Results and Discussion

Electrodeposition. Figure 1 shows a SEM micrograph of a typical layer deposited at pH 9 at room temperature on TFO. The layer consists of faceted crystals, indicating that the growth is kinetically rather than diffusion limited. The electrodeposited material was Cu_2O; only the expected peaks due to Cu_2O were present in the XRD spectra. The optical absorption spectra showed no absorption at wavelengths longer than 600 nm due to CuO. No changes in appearance or photoelectrochemical properties were found after keeping the Cu_2O layers in air for months. On the other hand, on annealing in a vacuum (pressure < 2×10^{-9} bar) at 400 °C for 12 h, the layer was reduced to copper.

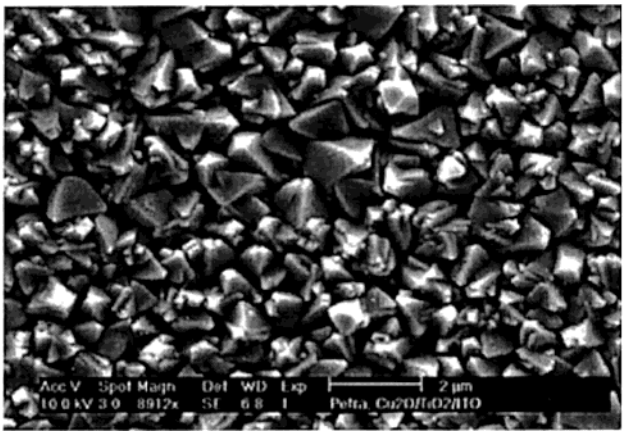

Figure 1. Cu_2O deposited on TFO at room temperature (current density 0.03 mA/cm^2; total charge 0.3 C/cm^2; pH 9).

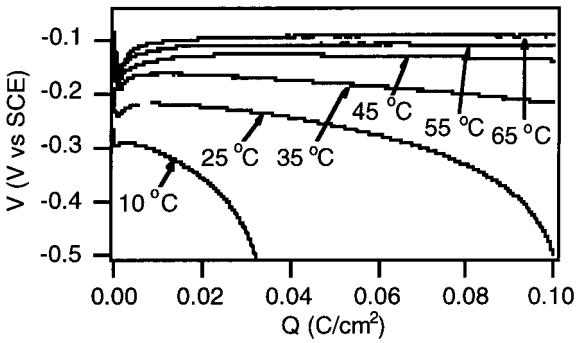

Figure 2. Potential−time transients during deposition at pH 9 with 0.05 mA/cm^2.

Figure 2 shows potential−time transients at different temperatures during galvanostatic deposition at pH 9. The current density was −0.05 mA/cm^2. The shape of the deposition curve clearly indicates a nucleation−growth mechanism. First, Cu_2O nuclei are formed on the bare substrate at a relatively negative potential. After a certain number of nuclei are formed, further growth of the layer is facilitated and the potential becomes less negative.

At low temperatures, a steady decrease in potential is seen during the growth of the layer. This is particulary evident at and below room temperature. If the potential becomes too negative, (e.g., for pH 9 at around −0.6 V), the potential starts to oscillate and Cu is codeposited.[22] This limits the maximum thickness of the pure oxide layers formed at room temperature under these conditions. At higher temperatures the potential needed for growth is less negative. Moreover, almost no decrease in potential is observed during growth. This means that higher current densities can be used and much thicker layers are possible. At 65 °C layers with a thickness up to a few micrometers can be formed. The marked differences between the curves in this limited temperature range indicate that the deposition involves a thermally activated process.

Figure 3 shows the logarithm of the deposition current density versus the inverse temperature for three potentials in a solution with pH 9. The activation energy, obtained from the Arrhenius plots, was 0.8 eV and

(21) de Jongh, P. E.; Vanmaekelbergh, D.; Kelly, J. J. Submitted for publication.

(22) Switzer, J. A.; Hung, C.-J.; Bohannan, E. W.; Shumsky, M. G.; Golden, T. D.; van Aken, D. C. *Adv. Mater.* **1997**, *9*, 334.

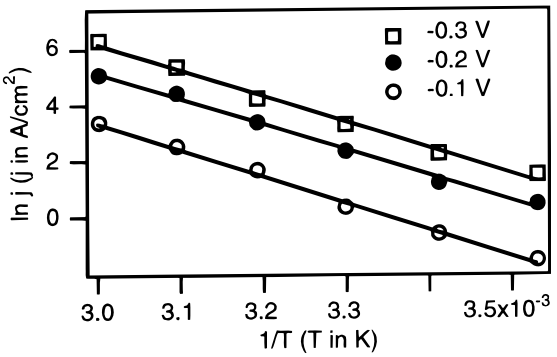

Figure 3. Logarithm of the deposition current density versus the inverse temperature for three potentials in a saturated Cu(II) lactate solution of pH 9.

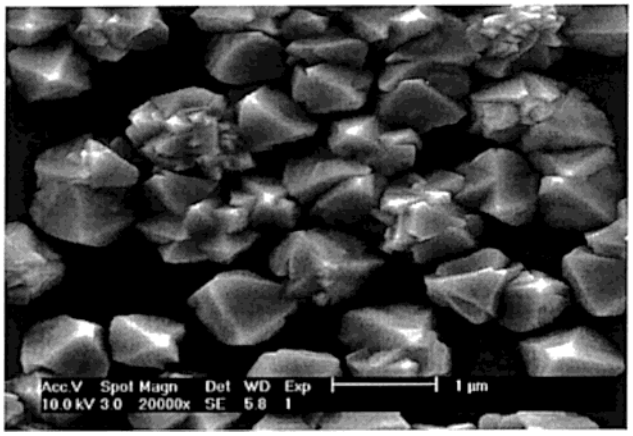

Figure 4. Cu_2O deposited at pH 9 (0.05 mA/cm^2; 0.1 C/cm^2; 55 °C).

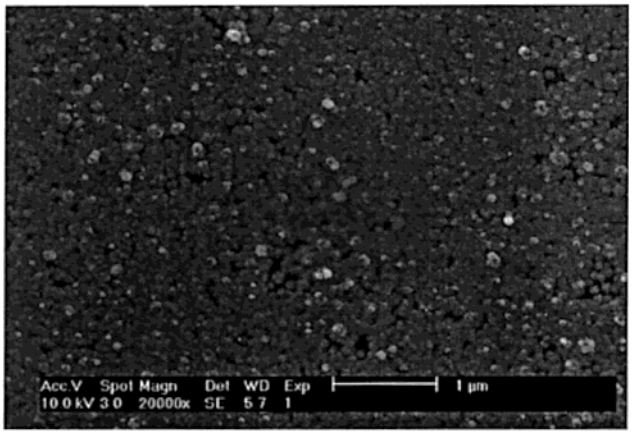

Figure 5. Cu_2O deposited at pH 9 (0.05 mA/cm^2; 0.1 C/cm^2; 10 °C).

independent of the applied potential. This value is in reasonable agreement with the activation energy of 0.6 eV found by Golden et al.[15]

The morphology of the crystals was strongly affected by the temperature. At pH 9, micrometer-sized crystals could be grown at 55 °C in the dark (Figure 4), while at 10 °C small crystallites were formed (Figure 5) for the same current density and deposition charge.

With galvanostatic deposition, changing the temperature to a lower value led to a more negative growth potential. However, if the temperature was restored to its initial value, the potential also returned to its original value. This reversibility indicates that the

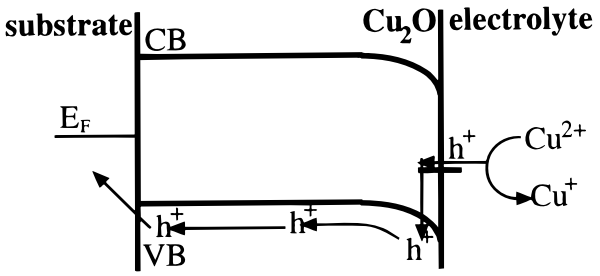

Figure 6. Deposition mechanism involving surface states and charge transport by holes inthe valence band.

influence of temperature is related to the kinetics of the growth process and is not due to the fact that the electrical properties of the material depend on the deposition temperature. The same was found for the influence of the current density on the growth potential.

Some conclusions can be drawn about the deposition mechanism. As Cu_2O is a p-type semiconductor, holes are the majority charge carriers. This means that the growth of large crystals is only possible via hole transport in the valence band. The position of the valence band is estimated to be at +0.6 V vs SCE at pH 7.[23] From the onset of the reduction of the Cu(II) lactate complex on TFO at pH 7 it can be concluded that the reduction potential is −0.1 V vs SCE or less negative. It is therefore unlikely that reduction of Cu(II) lactate takes place directly by hole injection into the valence band. Surface states probably play a role; the Cu(II) lactate complex injects a hole into a surface state in the Cu_2O, and the hole is subsequently excited thermally into the valence band. The hole travels through the valence band to the back substrate. This mechanism is schematically shown in Figure 6.

In this model, the activation energy of 0.8 eV that we found experimentally corresponds to the energy required to thermally excite a hole from a surface state into the valence band. A much lower value would be expected if the activation energy were due to a chemical reorganization of the Cu(II) lactate complex in solution. The activation energy was independent of the applied potential. This is consistent with the model if the surface states have a relatively narrow energy distribution and the position of both the band edges and the surface state shift with applied potential.

For low temperatures and small crystals another charge transport mechanism can play a role. As will be shown elsewhere the diffusion length of the minority charge carriers, electrons in the conduction band, is rather large, of the order of 10−100 nm.[21] This means that if the distance between the conducting substrate and the Cu_2O/electrolyte interface is within this range, it is possible that charge is carried by electrons in the conduction band. These can be trapped in surface states and subsequently reduce the Cu(II) lactate complex. At low temperatures, the valence band mechanism, involving a large activation energy, is less likely. The mechanism involving charge transport by electrons in the conduction band could then be predominant, explaining the small rounded particles formed at lower temperatures and the strong increase in negative potential when the particles reach a size more or less corresponding to

(23) Gerischer, H. *J. Electroanal. Chem.* **1977**, *82*, 133.

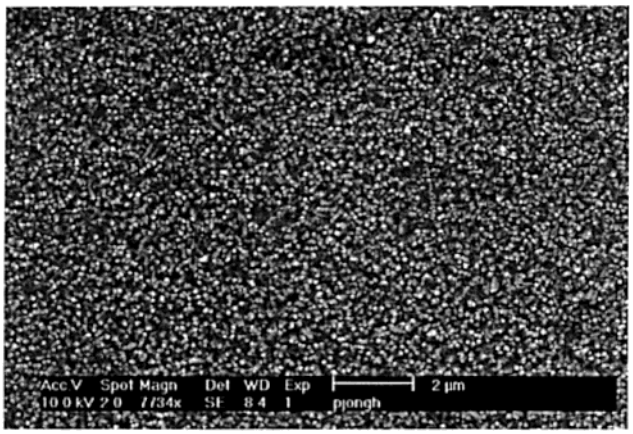

Figure 7. Cu_2O deposited at pH 11 (0.2 mA/cm^2; 0.13 C/cm^2; 55 °C).

the diffusion length of electrons in this material. This hypothesis is supported by the fact that at 10 °C, larger crystals can be grown if the electrode is illuminated.

The pH of the deposition solution had a strong influence on the morphology of the layers. At pH 7 and 8, copper was formed at higher current densities. For pH 9−12, well-defined layers of faceted Cu_2O crystals could be grown. At pH 13, the layer was spotty and large isolated crystals were formed. From the Pourbaix diagram it is known that Cu_2O is thermodynamically unstable outside the pH range 6−14 in aqueous environments.[24]

The nucleation process was strongly influenced by the pH: the higher the pH, the faster the nucleation. The nuclei density was determined by passing a small deposition charge, taking electron micrographs, and counting the average number of nuclei per unit surface area. At pH 11, the density of nuclei formed at a given deposition charge was more than an order of magnitude higher than at pH 8, leading to a morphology with relatively small crystals. Figure 7 shows a layer deposited at pH 11 and 55 °C.

The deposition efficiency was determined coulometrically by measuring the charge for Cu_2O deposition and subsequent anodic dissolution. From the ratio of dissolution to deposition, charge a value of about 0.9 was found. For thin layers the efficiency was lower. This high efficiency was confirmed by comparing the deposition charge with the layer thickness, which was determined with a surface profiler and from the interference patterns in the absorption spectra.

Optical Absorption. The color of the layers ranged from bright yellow to dark red depending on the thickness. Figure 8 (a) shows the absorption coefficient (α) as a function of the photon energy ($h\nu$), for a Cu_2O layer with an average thickness of 2.3 μm. The apparent absorption around 1.6 eV is due to interference in the layer, causing fringes over the whole spectrum. Absorption starts at 2.0 eV and rises only gradually with increasing photon energy up to about 2.5 eV. Above 2.5 eV, a sharper rise is seen. This initial slow rise and subsequent sharper rise at higher photon energies was found for all samples. Near the band gap energy, the absorption clearly does not increase as strongly with

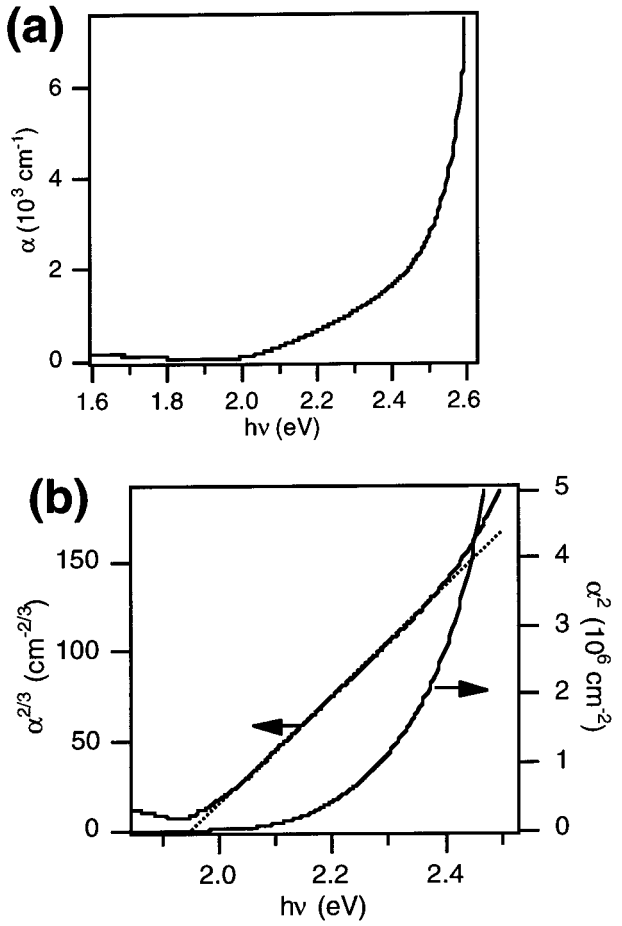

Figure 8. Effective absorption coefficient (α) versus the photon energy ($h\nu$) for a Cu_2O layer, deposited at pH 11 (0.2 mA/cm^2; 1.25 C/cm^2; 55 °C): (a) α vs $h\nu$ and (b) $\alpha^{2/3}$ and α^2 versus $h\nu$.

increasing photon energy as expected for a semiconductor with a direct allowed semiconductor.

The optical properties of Cu_2O have been intensively studied at low temperatures.[25−28] At 4 K, the optical transitions from the highest valence band to the lowest conduction band (the "yellow series", starting at 2.17 eV) are direct, but parity forbidden. The "green series" transitions from a band 0.13 eV lower than the highest valence band to the lowest conduction band, are also parity forbidden. The "blue series" transitions, starting at 2.62 eV, are parity allowed. Theoretically, for energies near the band gap, α should be proportional to $h\nu^{3/2}$ for forbidden direct transitions.[25,27]

In Figure 8b the absorption coefficient measured at room temperature is plotted as α^2 versus $h\nu$. A straight line is clearly not found for these photon energies. However, a plot of $\alpha^{2/3}$ versus $h\nu$ does give a straight line between 2.0 and 2.4 eV. From a fit of $\alpha^{2/3}$ versus $h\nu$ the band gap was estimated to be 1.96 eV. We should point out that also experimental α^2 and $\alpha^{1/2}$ vs $h\nu$ dependence are reported for the same spectral range.[13,15,26]

Cu_2O in Nanoporous TiO_2. Figure 9 shows the surface of a 1.5-μm-thick, nanoporous TiO_2 electrode,

(24) Pourbaix, M. *Atlas of Electrochemical Equilibria in Aqueous Solutions*; NACE: Houston, TX, 1974.

(25) Elliott, R. J. *Phys. Rev.* **1957**, *108*, 1384.
(26) Baumeister, P. W. *Phys. Rev.* **1961**, *121*, 359.
(27) Agekyan, V. T. *Phys. Status Solidi A* **1977**, *43*, 11.
(28) Washington, M. A.; Genack, A. Z.; Cummins, H. Z.; Bruce, R. H.; Compaan, A.; Forman, R. A. *Phys. Rev. B* **1977**, *15*, 2145.

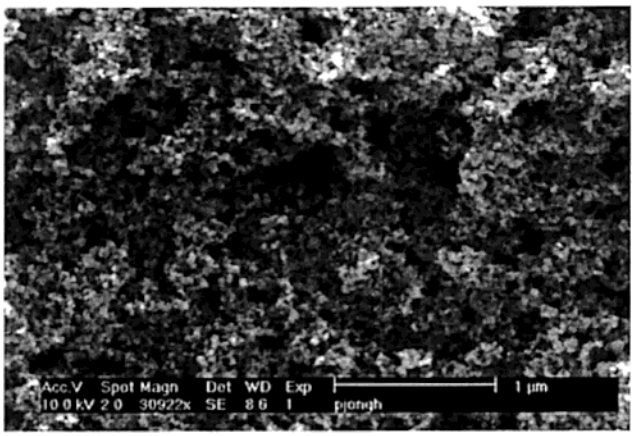

Figure 9. Nanoporous TiO_2 electrode consisting of 20−30-nm particles.

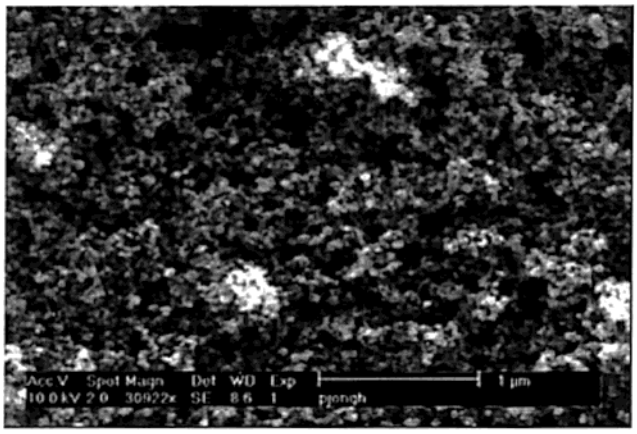

Figure 10. Cu_2O in TiO_2 (pore filling fraction 5%).

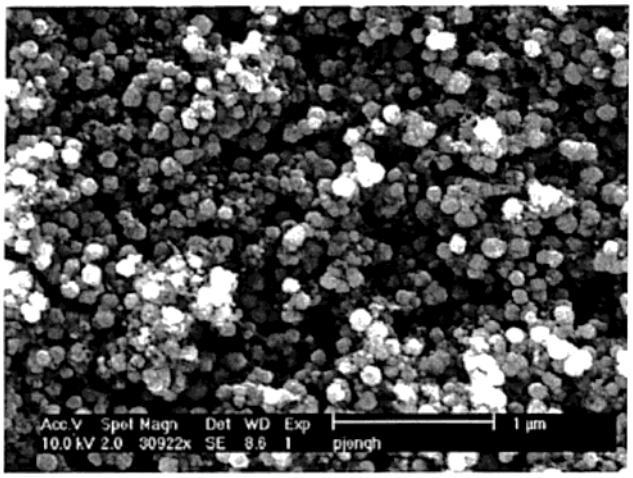

Figure 11. Cu_2O in TiO_2 (pore filling fraction 50%).

consisting of interconnected 20−30-nm particles on a conducting TFO substrate. The porosity of the electrode is 50−60%. Cu_2O could be electrodeposited inside these nanoporous electrodes. Figures 10 and 11 show two stages in the growth (note the different scales). An equivalent of 0.04 and 0.4 μm Cu_2O was deposited, corresponding to pore-filling fractions of about 5 and 50% respectively. Surprisingly, even for the 5% filling fraction already Cu_2O is seen in the upper part of the TiO_2 electrode. If filling fractions much higher than 50% were used, larger crystals were formed on top, as was seen by electron microscopy.

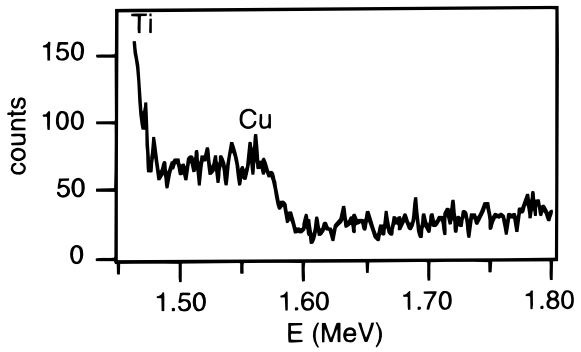

Figure 12. RBS spectrum on nanoporous TiO_2 filled with 5% Cu_2O.

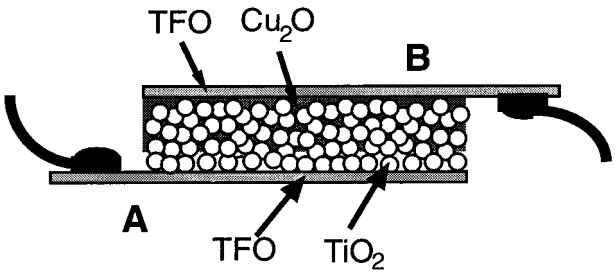

Figure 13. Schematic picture of the TFO−TiO_2−Cu_2O−TFO solid-state device.

The question was whether the Cu_2O was growing from the conducting substrate through the pores, or directly on the nanoporous TiO_2. We tried to deposit Cu_2O on single crystalline TiO_2, both in the dark under cathodic polarization, and under illumination. This proved impossible, only Cu was formed. To check whether the Cu_2O was growing uniformly through the layer or preferentially at the substrate/TiO_2 interface, RBS measurements were performed. A result for the electrode with 5% pore filling is shown in Figure 12. The onset energies for the detection of Cu and Ti at the surface are indicated. Between 1.57 and 1.47 MeV, the RBS signal is due only to Cu, this energy range corresponds to a depth of ~150 nm. The Cu_2O must therefore be deposited quite uniformly over this distance. The density of Cu atoms in this 150-nm layer corresponded to a pore-filling fraction with Cu_2O of about 6%, which is comparable to the average fraction over the whole electrode, calculated from the deposition charge. These results suggest that the Cu_2O is indeed distributed over the whole TiO_2 layer, instead of gradually filling the porous matrix from the conducting substrate outward, as might perhaps be expected. A substantial part of the Cu_2O could be reoxidized and dissolved anodically, implying that the oxide is coherent and in electrical contact with the conducting substrate. The TiO_2 was also not isolated from the conducting substrate, as both a cathodic photocurrent spectrum due to the Cu_2O and an anodic photocurrent spectrum due to the TiO_2 could be measured in an electrolyte solution.

To check for electrical contact between the Cu_2O and the TiO_2, we prepared a solid-state device, which is schematically shown in Figure 13. A nanoporous TiO_2 electrode filled with Cu_2O (side A in Figure 13) was pressed against a Cu_2O layer on TFO (side B). Some electrodeposition solution was infiltrated between the electrodes. The Cu_2O was dissolved galvanostatically from side A and electrodeposited onto side B. A sudden

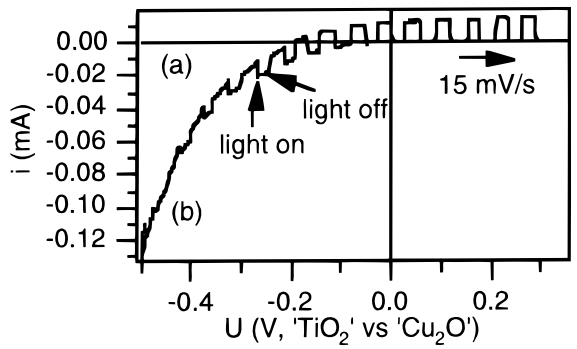

Figure 14. Current−voltage characteristics under chopped illumination of a TFO−TiO_2−Cu_2O−TFO solid-state device: (a) completely dry and (b) with a drop of water between the two electrodes.

change in potential indicated when all material was dissolved. Some further Cu_2O deposition on side B took place from the Cu(II) lactate solution inside the pores.

The solution had to be subsequently removed. This was done by first rinsing with water, then with ethanol, and drying under vacuum. It was very difficult to remove all liquid from the pores. Figure 14 shows the current−voltage characteristics under chopped, white illumination for this device. It is clear that if the cell is completely dry, no contact between the two electrodes was established. Electrical contact could not be obtained by annealing at 250 °C under air. After the cell was annealed at higher temperatures, short-circuiting was found. It does not seem possible to obtain direct electrical contact between the interpenetrated Cu_2O and TiO_2.

With a drop of water present between the two electrodes current−voltage characteristics resembling those of a photodiode were obtained. No current is found in the dark under reverse bias, while under forward bias an exponentially increasing current is observed. This current corresponds to the reduction of water on the n-type TiO_2 and oxidation of the p-type Cu_2O. Under reverse bias a photocurrent is found, corresponding to the oxidation of water on the TiO_2 electrode and a reduction reaction on the Cu_2O side by photogenerated charge carriers.

Conclusions

Well-defined, polycrystalline Cu_2O was electrodeposited on TFO conducting substrates. The temperature of the deposition solution, ranging from 10 to 65 °C, had a strong influence on the morphology of the oxide and on the deposition kinetics. At and below room temperature, a steady decrease in potential occurred during the deposition, limiting the thickness of the layers. Larger crystals could only be grown at higher temperatures.The pH of the solution also had a strong influence on the nucleation process and the morphology of the layers. On the basis of our results a model for the deposition was proposed.

The as-deposited Cu_2O is stable under ambient conditions. XRD and SEM measurements showed that the material did not contain Cu or CuO. The optical absoption in the visible was much weaker than expected for a semiconductor with a direct, allowed band gap transition of 2.0 eV. A composite material was made by electrodepositing Cu_2O inside a nanoporous TiO_2 electrode. It was not possible to obtain electrical contact between the p-type Cu_2O and n-type TiO_2.

Acknowledgment. I would like to thank Dirk Aarts and Henk Eshuis for their enthusiastic work on Cu_2O as part of a student project. Furthermore, I am grateful to Harold Kerp and Gert Hartman of the Surface Physics group in the Debye Institute, for performing the RBS measurements and providing a vacuum oven, respectively. The SEM micrographs were obtained at the Electron Microscopy Facilities of the Molecular Cell Biology department of Utrecht University.

CM991054E